06

On equations of state of nickel and a nickel-aluminum mixture at high pressures

© R.K. Belkheeva

Novosibirsk State University (NSU),
630090 Novosibirsk, Russia
e-mail: rimbel@academ.org, rumia@post.nsu.ru

Received May 11, 2025
Revised July 28, 2025
Accepted August 7, 2025

This study describes a method of constructing a Mie-Gruneisen equation of state with a small number of free parameters for nickel. It shows application of this equation of state for describing a behavior of the nickel-aluminum mixture. Porous samples of nickel and the nickel-aluminum mixture are considered as simple thermodynamic-equilibrium mixtures of a condensed substance and gas (air in the pores). Using a logarithmic dependence of the Gruneisen coefficient on a density made it possible to extend a range of applicability of the equations of state into a range of the lower densities. Hugoniot and Poisson adiabats for the nickel samples of various initial porosities and the porous samples of the aluminum-nickel mixture, which are calculated by means of this equation, well agree with experimental data. It is concluded that the proposed equation of state of nickel can be applied for describing the material behavior (including in the mixture with aluminum) under shock compression (not higher than 1 TPa) and isentropic expansion.

Keywords: equation of state, parameters of the equation of state, shock adiabat, unloading isentrope, thermodynamic equilibrium, Gruneisen coefficient

DOI: 10.61011/TP.2026.01.62849.110-25

Introduction

Demands of modern production require from science to solve problems of dynamic compaction, shock-wave synthesis of new materials and other explosive technologies. The mixtures differ by a large variety of the compositions and initial densities, whence it is required to construct a simple model of the equation of state, which takes into account the composition of and contributions by mixture components The study [1–11] describes some models of a various complexity degree for describing thermodynamics of the materials in a wide range of variation of pressures and densities in high-speed collision of bodies.

Nickel is a widely used material in metal doping, which characterizes its demand in industry. Information about nickel properties and its influence as a dopant on properties of alloys and mixtures is summarized in the study [12]. Describing the thermodynamic behavior of the mixtures and alloys requires equations of state.

The present study is aimed at determining parameters of the simple equation of state of nickel and constructing the equation of state of a mixture of several components as exemplified by the nickel-aluminum mixture at high pressures.

The thermodynamic properties of nickel are described by the studies [13–20], which have developed multi-phase equations of state taking into account three aggregate states of matter (solid, liquid and gaseous) and analyzed thermodynamic properties of metals that list nickel. The present study has constructed the equation of state of nickel based on the previously proposed model [21,22], which differs from [13–20] by simplicity and a small number of free parameters, but has a less broad applicability range up to pressures of at most 1 TPa. It is demonstrated that this equation of state can be used when describing thermodynamic properties of the nickel-aluminum mixture (for which the similar equation of state is constructed in the recent study [22]) under shock compression. The present study neglects transformation of a face-centered cubic (FCC) phase into a body-centered cubic (BCC) phase, which is discussed in theoretical studies [23–26], but not detected in shock-wave experiments.

1. Mathematical model of the equation of state

Many studies are dedicated to a task of selecting the equation of state for the condensed substance when describing shock-wave loading (for example, [1–11,13–22,27–30]). It is noted in these studies that the problem of theoretical calculation of the equation of state of the substance in the wide range of pressures and temperatures by statistics physics is extremely difficult. Therefore, we deal with simplified models that reflect only basic features of a phenomenon or process, thereby limiting the applicability range of the obtained equations of state. Among these approaches outstands a method of constructing semi-empirical models, which consists of pre-defining functional dependences of the thermodynamic parameters and using experimental

data for determining numerical values of coefficients. An applicability criterion of the equation of state is adequate description of a set of experimental data. Provided that the form (Mie-Gruneisen form) of pre-defining the equation of state of each component is the same, the study [31] proposes a method of constructing the equation of state of the N-component mixture. The paper [32] has substantiated application of the Mie-Gruneisen equation of state for air.

It is noted in the study [4,33] that when describing the behavior of the samples subjected to shock-wave compression, the Gruneisen coefficient can be described by the formula $\gamma = \gamma_0 r^{-l}$ (where $r = \rho/\rho_0$, ρ is a density; ρ_0 — a density under normal conditions; $l = \text{const}$, $l > 0$). In [34] is shown that when calculating the shock adiabats for highly-porous materials using this dependence for the Gruneisen coefficient results in its increase with growth of intensity of the shock wave. This is due to the fact that a final density of the shock-compressed sample turns out to be less than the normal density ($r^{-1} = \rho_0/\rho > 1$). The paper [21] has shown on the example of copper that use of an exponential function of the Gruneisen coefficient on the density with the exponent $l > 0$ for describing the highly-porous material does not agree with the experimental data. The paper [34] proposes to pre-define the dependence of the Gruneisen coefficient on the density with the formula $\gamma = \gamma_0 r^l$ (where $l = \text{const}$, $l > 0$) when describing the highly-porous substances and has compared results of calculations and experimental data for the samples of copper, iron and nickel with porosities exceeding 7.2.

In the paper [35], for the equation of state of several metals, including nickel, the Gruneisen coefficient is represented by an expression that can be easily reduced a form $\Gamma(T) = \Gamma_\infty + f(T)$, where

$$f(T) = \frac{\Gamma_0 - \Gamma_\infty}{1 + \beta T},$$

$\Gamma_0, \Gamma_\infty, \beta$ — free parameters, T — an absolute temperature. The paper [36] uses the following combination of approaches [34,35] for the equation of state of copper when describing the Gruneisen coefficient: a multiplier $r^{-\alpha}(1 + \beta T_0)$ is put in front of a summand $f(T)$ in the expression for the Gruneisen coefficient, where T_0 is a normal temperature. At the same time, in the compression region, the free parameter α is considered to be positive and in the tension region it is substituted with a negative free parameter δ. As a result, in the paper [36] the Gruneisen coefficient is pre-defined by a piecewise function

$$\Gamma(V, T) = \Gamma_\infty + r^{-\alpha}(1 + \beta T_0) f(T),$$

if $r > 1$ ($\alpha > 0$) and

$$\Gamma(V, T) = \Gamma_\infty + r^{-\delta}(1 + \beta T_0) f(T),$$

if $r < 1$ ($\delta < 0$). The Gruneisen coefficient pre-defined by these expressions is a continuous function of the volume, but a kink appears in the point $r = 1$. Consequently, a volume derivative of the Gruneisen coefficient is broken when $r = 1$:

$$\left(\frac{\partial \Gamma}{\partial V}\right)_T\Big|_{r\to 1, r>1} \neq \left(\frac{\partial \Gamma}{\partial V}\right)_T\Big|_{r\to 1, r<1},$$

since

$$\left(\frac{\partial \Gamma}{\partial V}\right)_T\Big|_{r\to 1, r>1} = \alpha\rho_0(1 + \beta T_0) f(T),$$

$$\left(\frac{\partial \Gamma}{\partial V}\right)_T\Big|_{r\to 1, r<1} = \delta\rho_0(1 + \beta T_0) f(T).$$

Therefore, pressure is also a continuous function, but the volume derivative of pressure is broken in the point $r = 1$. The paper [34] also pre-defines the Gruneisen function with a piecewise function. But since it studied the behavior of the heavily-porous materials, for which the sample densities did not exceed ρ_0 in a loading region, a derivative break in the point $r = 1$ ($\rho = \rho_0$), which is outside a region of consideration, did not affect the calculation results.

It is understood that using analytical functions, in particular, for describing the dependence of the Gruneisen coefficient on the density [11,28,37–42], excludes breaks in the thermodynamic parameters. The logarithmic dependence of a Gruneisen coefficient model on the density, which is proposed in the study [21]

$$\gamma = \gamma_0 r^{-\ln r} \tag{1}$$

makes it possible to avoid a case of the volume derivative of pressure, since in this case pressure is a smooth function of their variables. The dependence (1) extends the applicability region of the Gruneisen coefficient into low densities and makes it possible to adequately reflect an anomalous behavior of the shock adiabats when the heavily-porous samples are loaded. Since a logarithm sign depends on a value of the argument, when $r < 1$ the exponent becomes negative and the values of γ decrease when intensity of the shock wave increases.

In the present study the porous N-component mixture is considered as a heterogeneous medium, whose pores are filled with air. The porosity (m) is understood as a ratio of the normal density of a monolith (ρ_{T0}) to the initial density of the porous sample (ρ_{00}). Excluded from consideration in the present study are effects related to thermal excitation of an electron subsystem, melting evaporation and ionization. High pressures occurring when strong shock waves propagate make it possible to neglect strength-related effects and use conditions of a phase pressure equality as conditions of joint motion [43]. At this, when the effects of relative motion of the components are insignificant and the mixture is in thermodynamic equilibrium, the following conditions are met $P_i = P$, $T_i = T$, $u_i = u$ (where P_i, T_i, u_i — pressure, temperature and mass speed of the component i; P, T, u is pressure, temperature and mass speed of the mixture as a whole). Then, motion of this medium can be described as motion of a single continuum with a special equation of state which takes into account properties of the mixture components and their mass fractions, thereby resulting

in significant reduction of the number of the equations. Within a framework of such a method of mixture, it is assumed that the equations of state of the components in the medium are the same as in a free state. For simple mixtures which do not form bonds in an atomic scale, the paper [43] describes the principles of constructing the model of interacting and interpenetrating continuums. The method of describing the mixture by a single continuum has been previously considered, for example, in the studies [43–45]. Within the framework of this method of describing a mixture of continuums in thermodynamic equilibrium, the studies [21,34] describe explain a method of constructing the equation of state of an equilibrium N-component mixture and specify ratios for calculating parameters of the equation of state of the mixture $A, n, \rho_0, \gamma_0, c_{V0}$ via parameters and mass portions (x_i) of the components.

It is noted in the study [1] that when describing the shock-wave phenomena a behavior of the condensed substances can be simulated by the Mie-Gruneisen equation of state, which represents pressure P as a sum of summands describing cold compression (P_X) and a temperature dependence (P_T):

$$P = P_X + P_T. \tag{2}$$

The present study represents the summands of full pressure (2) with the following expressions

$$P_X = A\lfloor r^n - 1\rfloor - \gamma r \rho_0 c_{V0} T_0, \tag{3}$$

$$P_T = \gamma r \rho_0 c_{V0} T. \tag{4}$$

Here $r = \rho/\rho_0$; ρ_0 is a parameter of the equation of state (in case of the condensed substance it is its density under the normal conditions; A, n are constants that characterize the substance; γ is the Gruneisen coefficient; c_{V0} is specific heat capacity at the constant volume (c_{V0} is assumed to be constant in the present study); $T_0 = 293\,\mathrm{K}$. The parameters n and A are interrelated by a relationship

$$A = \frac{c_0^2 \rho_0}{n},$$

where c_0 is a volume speed of sound under the normal conditions. In this case, the equation of state (2) is written as

$$P = A\lfloor r^n - 1\rfloor + \gamma_0 \rho_0 r^{1-\ln r} c_{V0}(T - T_0).$$

Internal energy is also represented as a sum of two summands:

$$E = E_X + E_T, \tag{5}$$

where E_X and E_T is an elastic and a thermal part of the internal energy, respectively.

$$E_X = \frac{A}{(n-1)\rho_0}[r^{n-1} - 1] + \frac{A}{\rho_0}[r^{-1} - 1]$$

$$- \gamma_0 c_{V0} T_0 \frac{\sqrt{\pi}}{2} \operatorname{erf}(\ln r) - c_{V0} T_0, \tag{6}$$

$$E_T = c_{V0} T. \tag{7}$$

Here we use an error function

$$\operatorname{erf}(x) = \frac{2}{\sqrt{\pi}} \int_0^x \exp(-t^2) dt,$$

for which the study [37] provides an approximation expression that makes it possible to calculate its values with quite high accuracy.

As in some other known studies (for example, [47–49]), the previous studies of the author [21,31,32,34,46] did not focus on the fact that thermodynamic consistency of the equations (2) and (5) requires to select formulas for the summands in (2) and (5) so that they satisfy the main thermodynamic identity [1]; the summand $\gamma \rho c_{V0} T_0$ shall be added to the cold part of pressure.

The study [21] uses only one free parameter (γ_0) for describing the thermal part of pressure by means of (1) and just two free parameters (n and γ_0) for the entire model of the equation of state.

When calculating for copper, the study [21] pre-defined that $\gamma_0 = 2$ for the expression (1). The equation of state with such a Gruneisen coefficient well described the behavior of the materials with low (below 3) and high porosity (above 5.4, when the shock adiabats exhibit an anomalous progress, in which the samples in the shock wave are compressed to densities that are the less the higher pressure, in a certain range of pressures). The present study describes selection of the value of γ_0, which makes it possible to described the whole spectrum of porosities.

When using the expression (1), with the compression ratios ρ/ρ_{T0} of about 3 the value of the Gruneisen coefficient becomes less than a commonly-accepted value of 2/3. In order to decelerate a rate of decreasing of the Gruneisen coefficient, another parameter α can be introduced to describe it:

$$\gamma = \gamma_0 r^{-\alpha \ln r}. \tag{8}$$

The method described in the study [21] was used for the equation of state of the mixture as written in (2)–(4), whose Gruneisen coefficient is pre-defined as (8), to obtain relationships for calculating parameters of the equation of state of the mixture via the respective parameters and mass portions of the components:

$$n = \frac{S_1 S_3}{S_2^2} - 1, \; A = kA_{\max} - \frac{nS_2}{S_1},$$

$$\rho_0 = \frac{1}{S_1}\left(\frac{A}{P + kA_{\max}}\right)^{1/n}, \; \alpha = \frac{1}{\ln(\rho_0 S_1)}\left(\frac{S_1 S_5}{S_2 S_4} - 1\right),$$

$$\gamma_0 = \frac{nS_4}{c_{V0}} (\rho_0 S_1)^{\alpha \ln(\rho_0 S_1)}, \; c_{V0} = \sum_{i=1}^{N} x_i c_{V0i}, \tag{9}$$

where

$$S_1 = \sum_{i=1}^{N} R_i, \; S_2 = \sum_{i=1}^{N} R_i \frac{kA_{\max} - A_i}{n_i},$$

$$S_3 = \sum_{i=1}^{N} R_i (n_i + 1) \left(\frac{kA_{\max} - A_i}{n_i} \right)^2,$$

$$S_4 = \sum_{i=1}^{N} R_i^{-\alpha_i \ln R_i} \frac{\rho_{0i} c_{V0i} \gamma_{0i}}{n_i},$$

$$S_5 = \sum_{i=1}^{n} R_i^{-\alpha_i \ln R_i} \frac{\rho_{0i} c_{V0i} \gamma_{0i}}{n_i} \frac{kA_{\max} - A_i}{n_i} (1 + \alpha_i \ln R_i),$$

$$R_i = \frac{x_i}{\rho_{0i}} \left(\frac{A_i}{P + kA_{\max}} \right)^{1/n_i}.$$

Here $A_i, n_i, \rho_{0i}, \gamma_{0i}, \alpha_i, c_{V0i}$ are parameters of the equations of state (the compression coefficient, the compression index, the normal density, the constant parameters of the Gruneisen coefficient, the specific heat capacity at the constant volume) of the component i; $A_{\max} = \max\{A_1, \ldots, A_N\}$. It is shown in the study [34] that when the value $k = 2$ a convergence condition is fulfilled when obtaining the relationships (9). These relationships are obtained provided that the equations of state of the components are pre-defined in the same form. In this case, instead of (6) the expression for the elastic part of energy is written as

$$E_X = \frac{A}{(n-1)\rho_0} [r^{n-1} - 1] + \frac{A}{\rho_0} [r^{-1} - 1] - \gamma_0 c_{V0} T_0 \frac{\sqrt{\pi}}{2\sqrt{\alpha}} \operatorname{erf}(\sqrt{\alpha} \ln r) - c_{V0} T_0. \quad (10)$$

Thus, we have constructed the simple small-parameter model of the equation of state of the thermodynamic-equilibrium N-component mixture (2)–(5), (7)–(10).

The parameters of the equation of state for the mixture, which are obtained by means of the relationships (9), depend on a current value of pressure P. It is shown in the study [46] for the case when $\alpha = 1$ that the equation of state of the mixture with parameters obtained using the relationships (9) when $P = 0$ (under the normal conditions) adequately describes the behavior of the mixture both when loading and unloading. Results of the calculations performed with the constant values of the parameters of the equation of state of the mixture make almost no difference from results of the calculations performed with parameters depending on current pressure. The present study's calculations are performed with constant values of the parameters of the equation of state of the mixture, which are calculated when $P = 0$. Description of shock-wave loading of the porous samples of nickel and the porous samples of the nickel-aluminum mixture requires to obtain the two free parameters (n and γ_0) for the equation of state of nickel. The parameter α was not selected in the present study. This parameter can be selected due to availability of experimental data under high-intense loading of the samples. The calculated shock adiabats and unloading isentropes for the two pre-defined values of α were compared with the experimental data.

It is noted in the study [1] that zero values can be taken as a start of counting of pressure and internal energy when calculating the behavior of solid bodies under high pressures. The Hugoniot equations for the initially still medium when the pressure in the unperturbed medium is zero are as follows

$$\rho_{00} D = \rho (D - u), \; P = \rho_{00} D u, \; E - E_0 = \frac{P}{2} \left(\frac{1}{\rho_{00}} - \frac{1}{\rho} \right), \quad (11)$$

where ρ_{00}, E_0 is the density and specific internal energy of the mixture upstream of a shock-wave front, respectively; u, P, ρ, E are a mass speed, pressure, density and specific internal energy of the medium downstream of the shock-wave front; D is a speed of the shock-wave front. Supplementing the relationships (11) with the equations of state of the medium (2)–(5), (7), (8), (10) and formulas for calculating the mixture parameters (9) results in a system of equations for unknown u, D, E, P, ρ. By defining the value of the mass speed of the medium downstream of the shock-wave front, it is possible to determine values of all the desired magnitudes.

Values of the parameters, which were used when calculating shock-wave compression and isentropic unloading of the samples, are given in Table (for aluminum, the values of the constants are taken from the study [22], so for air are they from the study [32]).

2. Calculation results and comparison with the experiment

Section 2 describes a method of selecting the parameters n and γ_0 for the equation of state of nickel based on the model of the mixture [21,22] and the Gruneisen coefficient in the form of (8) in order to describe the behavior of this metal and its mixture with aluminum under shock compression and isentropic unloading. Besides, the second parameter is used ($\alpha \neq 1$; the studies [21,22] considered only an option when $\alpha = 1$) for describing the Gruneisen coefficient. When selecting γ_0, one should take into account that the influence of this parameter is most pronounced when describing almost vertical adiabats in the coordinates „compression ratio — pressure“. In this case, the value of $r = \rho/\rho_0$ is close to unity and a contribution by the cold component P_X to pressure is almost zero. Available experimental data are taken for nickel to select the adiabats for the samples with porosities $m = 2.305, 2.706, 3.0$. It is clear by results in Fig. 1 that the adiabats calculated with the value $\gamma_0 = 1.55$ deviate to the right from the experimental dots [50] and when calculated with the value $\gamma_0 = 1.75$ they deviate to the left therefrom. The study selects the only value of γ_0, which will be used for calculating the shock adiabats for the samples with all the values of porosities. Therefore, the value $\gamma_0 = 1.63$ is selected, at which the calculated shock adiabats marked with unprimed digits agree with the experimental data [50] both for $m = 2.305$ and $m = 2.706$.

Parameters of the equation of state of nickel, aluminum and air

Substance	ρ_{0i}, kg/m^3	c_{0i}, km/s	n_i	c_{V0i}, kJ/(kg · K)	γ_{0i}	α_i
Nickel	8875	4.65	4.1	0.442	1.63	1
Nickel	8875	4.65	3.70	0.442	1.63	0.5
Aluminium	2712	5.33	3.46	0.8975	1.65	1
Air	1.3	0.343	2.20	0.718	0.16	1

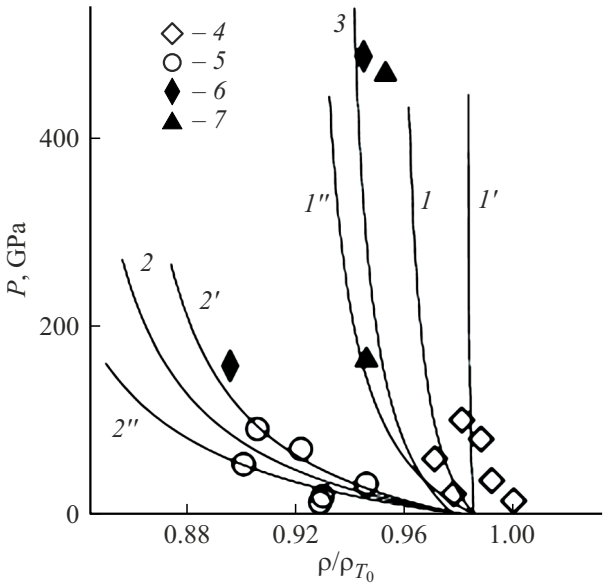

Figure 1. Pressure (P) as a function of the compression ratio (ρ/ρ_{T0}) on the shock adiabats of nickel for initial porosities $m = 2.305$ (*1, 1′, 1″*), 2.706 (*2, 2′, 2″*) and 3.0 (*3*); $\gamma_0 = 1.63$ (*1, 2*), 1.55 (*1′, 2′*), 1.75 (*1″, 2″*), and 1.1 (*3*); the experimental data: *4* — $m = 2.305$ [50]; *5* — $m = 2.706$ [50]; *6* — $m = 3.0$ [50]; *7* — $m = 3.0$ [51]; $\rho_{T0} = 8.875\,\text{g/cm}^3$.

In order to refine the value of γ_0 for porosity $m = 3$, the expression for the shock adiabat is provided as obtained from the third equation of the system (11):

$$P = \frac{(h-1)P_X - 2\rho(E_X - E_0)}{h - \rho/\rho_{00}},\ h = \frac{2}{\gamma} + 1. \qquad (12)$$

It is clear that the behavior of almost vertically arranged points [50,51] for $m = 3$ can be described by the expression (12) if a fraction denominator is close to zero. Taking into account that when $m = 3$, $\rho \approx \rho_{T0}$, $m = \rho_{T0}/\rho_{00}$, we obtain that the value of γ_0 is close to unity. The value of γ_0, which is 1.1, is assumed to be a special solution. Hereinafter, the value of γ_0 is assumed to be 1.63 for all porosities except for $m = 3$. The parameters of the equation of state, which are calculated by the formulas (9), depend on mass concentrations of the components and current pressure. As a result, the initial values of the parameter ρ_0 (when $P = 0$) for the mixture of the condensed and the gaseous substance are shifted to the left with an increase of porosity, which is visibly observed in Fig. 1.

Fig. 2, *a* shows graphs of a dependence of the Gruneisen coefficient on the compression ratio, which is pre-defined by the formula (8), when the values of the parameter $\alpha = 1$ and 0.5 on the shock adiabat of the initially solid samples of nickel. Since when $\alpha = 0.5$ a portion of the thermal component in pressure (P_T) increases, then, accordingly, a portion of elastic pressure (P_X) decreases. This fact is taken into account by pre-defining the compression index n. In Fig. 2, *a*, a limit right value of the compression ratio, which is 7.45 ($\rho/\rho_{T0} = 7.45$), is obtained for $\alpha = 1$ when the pressure values $P \approx 192.9$ TPa and for $\alpha = 0.5$ when $P \approx 268.4$ TPa.

Fig. 2, *b, c*, 3, 4 shows results of calculations of the shock adiabats and unloading isentropes when $\alpha = 1$ and 0.5. The calculated adiabats for the solid samples, which are calculated with the values of the parameters of the equation of state with $\alpha = 1$ and 0.5, and the experimental data [50–57] are compared in Fig. 2, *b, c* in the coordinates u–D and ρ/ρ_{T0}–P, respectively. A divergence of the calculated curves increases with an increase of intensity of the shock wave. It is compared to show that up to the mass speeds $u \approx 8$ km/s, the compression ratios of about 2 and pressures of 1 TPa both the curves are almost identical to each other and well agree with the experimental data [50–57].

The calculated and experimental [50,58,59] shock adiabats for the various-porosity samples of nickel are compared in Fig. 3, *a* in the coordinates u–D and in Fig. 3, *b* in the coordinates ρ/ρ_{T0}–P. The curves calculated by means of the proposed equation of state with the Gruneisen coefficient pre-defined by the relationship (8) well agree with the experimental data [50,58,59].

The study [60] has proposed two potentials of a submerged-atom model for the FCC and BCC phases of nickel; detected parameters of these potentials by properties of a metal on the isobar and the shock adiabat; calculated a nickel melting line and specified coordinates of a melting area on the shock adiabat for solid nickel: for pressure 275.8–297.6 GPa, for the temperature 4422–4499 K; compared with data of the other authors, which are different from those of the study [60] (see references in the study [60]). Under shock-wave loading of the porous samples, the temperatures are higher, the higher porosity and melting in the porous samples starts at pressures below 275.8 GPa. Ranges of variation of pressures and temperatures when melting are insignificant as compared to achieved values of these magnitudes. It is shown in the study [61] that a substance melting effect in the shock wave

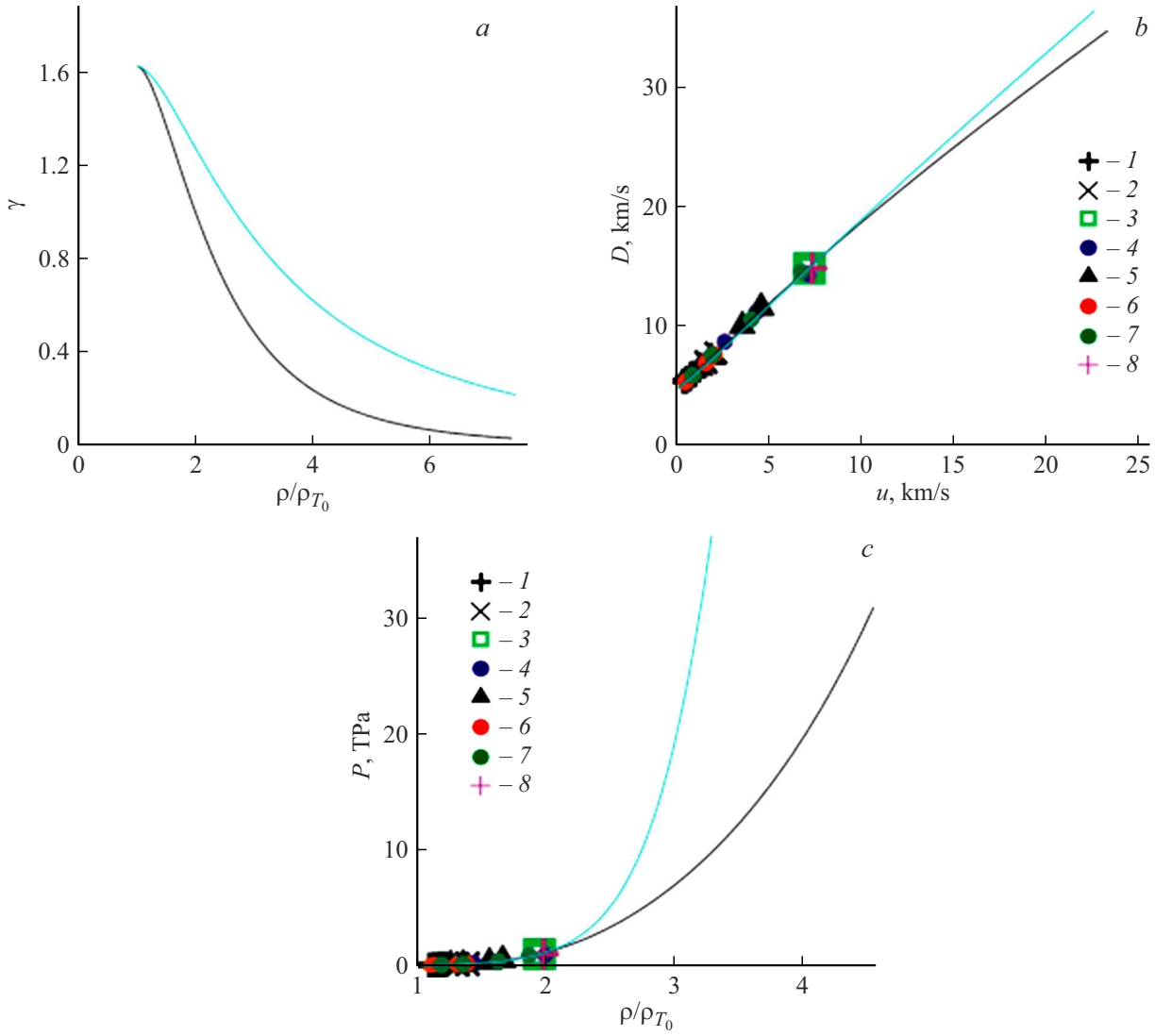

Figure 2. Shock adiabats of the initially solid samples of nickel when $\alpha = 1$ (the black lines) and 0.5 (the light-blue lines): *a* — the dependences of the Gruneisen coefficient (γ) on the compression ratio (ρ/ρ_{T0}); *b* — the wave speed (D) as a function of the mass speed (u); *c* — pressure (P) as a function of the compression ratio (ρ/ρ_{T0}). The experimental data: *1* — [52]; *2* — [53]; *3* — [51]; *4* — [54]; *5* — [55]; *6* — [56]; *7* — [57]; *8* — [50].

is hardly noticeable on the shock adiabats for the aluminum samples of the various initial density. It is assumed in the present study that for the other substances, including for nickel, taking into account melting makes neither influence on the form of the shock adiabat in the coordinates specified in Fig. 2, *b, c* and 3. The calculated and experimental shock-wave data for the solid and porous nickel samples up to pressures of 1 TPa are compared in Fig. 2, *b, c* (for the solid samples) and Fig. 3 to conclude that the proposed equation of state of nickel can be applied within the said range of pressures.

The unloading isentropes shown in Fig. 4 in the coordinates $u-P$ show good coincidence of results of the calculations and the experimental data [62] except for the points when pressure $P < 0.1$ GPa, i.e. in the area of the liquid–vapor phase transition that is not taken into account in the represented simple model.

Assuming that the experimental date are exact, for the small values of r $(0.945 < r < 1.371)$ the study [63] divides a compression space downstream of the shock-wave front into subintervals of the width $\Delta r = 0.04$ and from an experimental database [64,65] it selects data related to these narrow intervals. Assuming that the Gruneisen coefficient $\gamma = V(\partial P/\partial E)_V$, coefficients of a slope $(\partial P/\partial E)_V$ of the curves (that are plotted by the experimental data for porosities $1 \le m \le 3$ in the coordinates $\Delta E-P$), where ΔE is an energy jump, P is shock-wave pressure, are used to estimate the Gruneisen coefficient in the shock wave. According to the set of data in these ranges of porosities and compressions in the study [63], the Gruneisen

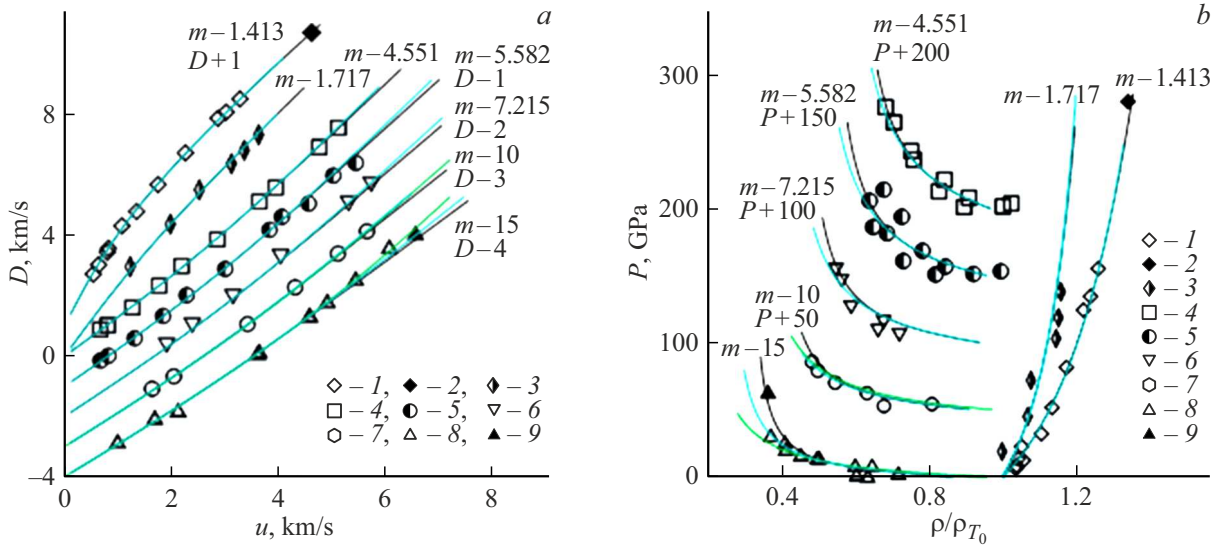

Figure 3. Shock adiabats of the various-porosity samples of nickel when $\alpha = 1$ (the black lines) and 0.5 (the light-blue lines) as well as according to the model [34] (the green lines): *a* — the wave speed (D) as a function of the mass speed (u); *b* — pressure (P) as a function of the compression ratio (ρ/ρ_{T0}). The curves include the values of porosities and values of the shift of the wave speed and pressure nearby. The experimental data, *m*: *1* — 1.413 [50]; *2* — 1.427 [50]; *3* — 1.717 [50]; *4* — 4.551 [50]; *5* — 5.582 [50]; *6* — 7.215 [50]; *7* — 10 [58]; *8* — 15 [58]; *9* — 15 [59].

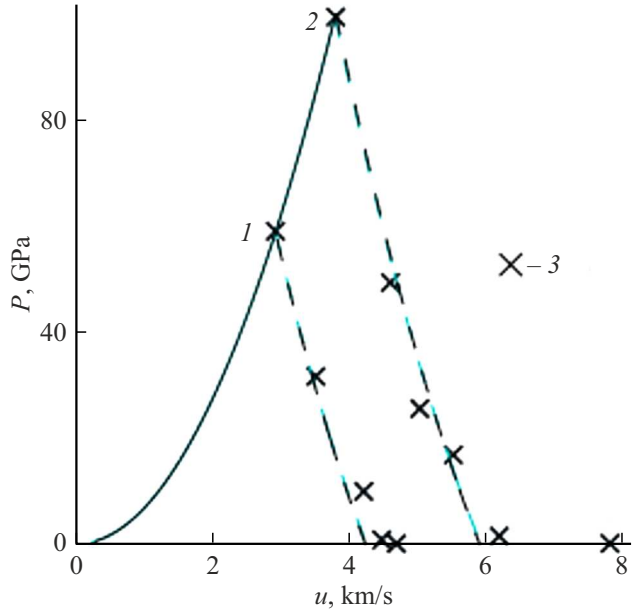

Figure 4. Pressure (P) as a function of the mass speed (u) on the shock adiabat (the solid line) and unloading isentropes (the dashed lines) of the shock-compressed samples of nickel of initial porosity $m = 2.305$ when $\alpha = 1$ (the black lines) and 0.5 (the light-blue lines). Experimental data: *3* — [62]. In the point *1* — $u = 2.91$ km/s, $P = 59$ GPa, in the point *2* — $u = 3.78$ km/s, $P = 99.4$ GPa.

coefficient varies within the range $1.64 > \gamma > 0.97$ and it varies within $1.64 > \gamma > 0.6$ according to the molecular-dynamic results [66]. The results of the calculations [63] noticeably differ from those in the study [66] and with a growth of porosity the divergence increases.

Fig. 5 shows dependences of the Gruneisen coefficient, which are obtained herein for the respective ranges of compression and porosity. According to an estimate of the study [63], for porosities below 1.744, the Gruneisen coefficient varies within the range $1.61 \geq \gamma \geq 0.91$, while in Fig. 5 it varies within the range $1.65 > \gamma > 1.45$ when $\alpha = 1$ and within the range $1.65 > \gamma > 1.55$ when

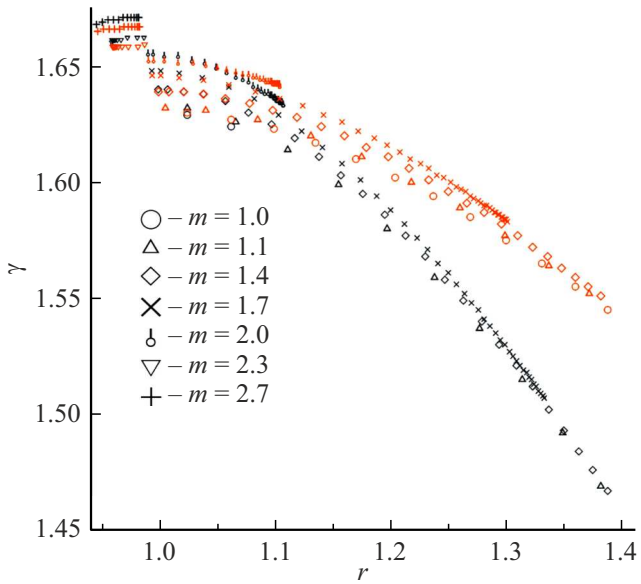

Figure 5. Calculated dependences of the Gruneisen coefficient on the compression ratio in the shock wave for $\alpha = 1$ (the black symbols) and 0.5 (the red symbols).

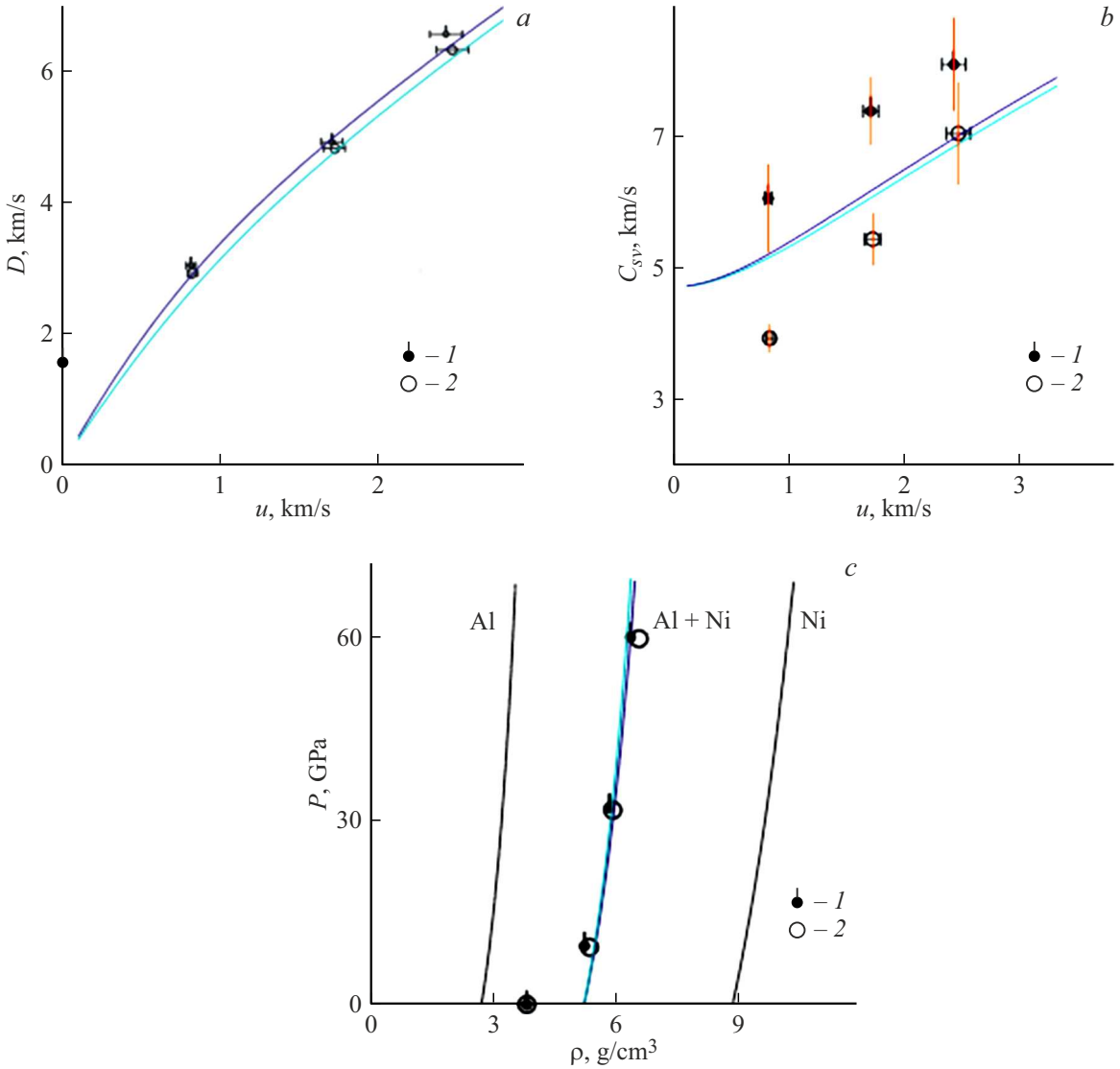

Figure 6. Shock adiabats of the samples of the Al(0.315)Ni(0.685) mixture with $\rho_{00} = 3.75$ (the light-blue lines) and 3.92 g/cm^3 (the deep-blue lines) as well as for the samples of aluminum (Al) and nickel (Ni) with initial porosity $m = 1.35$ (the black lines): *a* — the wave speed (D) as a function of the mass speed (u) (*1, 2* — the experimental data [67]); *b* — the speed of sound (C_{vs}) as a function of the mass speed (u) (*1, 2* — the experimental data [68]); *c* — pressure (P) as a function of the density (ρ) (*1, 2* — the experimental data [67]).

$\alpha = 0.5$. For porosities $m \geq 2$, according to the estimate of the study [63] $1.6 > \gamma > 0.97$, while herein for porosity $m = 2$ the Gruneisen coefficient varies within the range $1.66 > \gamma > 1.63$ when $\alpha = 1$ and within the range $1.66 > \gamma > 1.64$ when $\alpha = 0.5$.

The studies [67,68] have experimentally studied shock compressibility of a mixture of micro- and nano-dispersed powders of aluminum (the mass fraction $x_{\mathrm{Al}} = 0.315$) and nickel (the mass fraction $x_{\mathrm{Ni}} = 0.685$) and measured the speed of sound downstream of the shock-wave front in order to determine whether a reaction with formation of nickel aluminide can proceed. The obtained experimental data and the results obtained using the proposed equation of state of the mixture are compared in Fig. 6. The parameters when $\alpha = 1$ were used for the equation of state of nickel. In the studies [67,68], the initial densities of powder-pressed samples were assumed to have the values 3.75–3.92 g/cm^3. Fig. 6 shows the calculated shock adiabats for the Al(0.315)Ni(0.685) mixture. Fig. 6, *c* also shows the shock adiabats for the nickel and aluminum samples with porosity $m = 1.35$, which corresponds to initial porosity of the samples of the aluminum-nickel mixture in the experiment [67,68].

The graphs in Fig. 6, *a, c* show good agreement of the calculated curves and the experimental data [67]. The differences in Fig. 6, *b* are due to melting of the samples in the tests [68]. It is noted in the study [68] that the micro- and nano-dispersed nickel samples start melting when $P = 30$

and at 37 GPa they turn out to be totally melt; while the aluminum samples start melting when $P = 47$ and at 60 GPa they turn out to be totally melt. This is the difference between the calculated results of the author (the phase transitions are not taken into account) and the data [67,68].

Conclusion

Nickel is exemplified to show the method of selecting the parameters for the Mie-Gruneisen small-parameter equation of state, which reliably describes the behavior of the solid and porous samples of nickel and the nickel-aluminum mixture under shock compression and isentropic unloading. The new expression (8) for the Gruneisen coefficient (with the additional parameter α) makes it possible to extend the application range of the previously proposed model to the parameters that are achieved when loading the samples of high values of initial porosity (up to $m \approx 15$). The results of comparing the calculated and experimental shock adiabats for the nickel sample of various initial porosities show good description of the behavior of nickel (including in the mixture with aluminum) in the shock waves of intensity of at most 1 TPa within the framework of the proposed equation of state (with the selected parameters n and γ).

Acknowledgments

The author would like to thank V.V. Yakushev for provided experimental data.

Conflict of interest

The author declares that he has no conflict of interest.

References

[1] Ya.B. Zel'dovich, Yu.P. Raizer, *Fizika udarnykh voln i vysokotemperaturnykh gidrodinamicheskikh yavlenii* (Nauka, M., 1966) (in Russian).
[2] R.G. McQueen, S.P. Marsh, J.W. Taylor, J.N. Fritz, W.J. Carter. In: R. Kinslow (editor). *High Velocity Impact Phenomena* (Academic Press, NY., 1970), p. 293.
[3] P. Caldirola, H. Knoepfel (editors). *Physics of High Energy Density* (Academic Press, NY., 1971)
[4] A.V. Bushman, V.E. Fortov. Phys. Usp., **26** (6), 465 (1983). DOI: 10.1070/PU1983v026n06ABEH004419
[5] S. Elieser, A.K. Ghatak, H. Hora. *An Introduction to Equations of State: Theory and Applications* (Cambridge Univ. Press, Cambridge, 1986)
[6] A.V. Bushman, G.I. Kanel', A.L. Ni, V.E. Fortov. *Teplofizika i dinamika intensivnykh impul'snykh vozdeistvii* (OIKhF, Chernogolovka, 1988) (in Russian).
[7] A.V. Bushman, I.V. Lomonosov, V.E. Fortov. *Uravneniya sostoyaniya metallov pri vysokikh plotnostyakh energii* (IKhFCh, Chenogolovka, 1992) (in Russian).
[8] V.M. Fomin, A.I. Gulidov, G.A. Sapozhnikov, I.I. Shabalin. *Vysokoskorostnoe vzaimodeistvie tel* (SO RAN, Novosibirsk, 1999) (in Russian).
[9] V.E. Fortov, L.V. Al'tshuler, R.F. Trunin, A.I. Funtikov (red.). *Udarnye volny is ekstremal'nye sostoyaniya veschchestva* (Nauka, M., 2000) (in Russian).
[10] K.V. Khishchenko, A.E. Mayer. Int. J. Mech. Sci., **189**, 105971 (2021).
[11] K.V. Khishchenko. TVT, **61** (3), 477 (2023) (in Russian). DOI: 10.31857/S0040364423050071
[12] I.L. Knunyants (red.). *Khimisheskaya entsiklopediya v pyati tomakh* (Sovetskaya entsiklopediya, M., 1988), t. 3 (in Russian).
[13] I.V. Lomonosov, V.E. Fortov, K.V. Khishchenko, P.R. Levashov. AIP Conf. Proc., **505**, 85 (2000).
[14] P.R. Levashov, V.E. Fortov, K.V. Khishchenko, I.V. Lomonosov. AIP Conf. Proc., **505**, 89 (2000).
[15] I.V. Lomonosov, V.E. Fortov, K.V. Khishchenko, P.R. Levashov. AIP Conf. Proc., **620**, 111 (2002).
[16] G.I. Kerley. *Equations of State for Be, Ni, W, and Au. Report SAND2003-3784* (Sandia National Laboratories, Albuquerque, NM, 2003)
[17] K.V. Khishchenko. *34th European Physical Society Conference on Plasma Physics, July 2–6, 2007, Warsaw, Poland*. Europhysics Conference Abstracts, **31F**, P-2.121 (2007)
[18] A.B. Medvedev, R.F. Trunin. Phys. Usp., **55**, 773 (2012).
[19] I.V. Lomonosov, V.K. Gryaznov. Contrib. Plasma Phys., **56** (3–4), 302 (2016).
[20] C.J. Prisbrey, P. Söderlind, C.J. Wu. AIP Conf. Proc., **3066**, 500012 (2024.)
[21] R.K. Belkheeva. High Temp., **60** (1), 26 (2022). DOI: 10.1134/S0018151X21040040
[22] R.K. Bel'kheeva. ZhTF, **95** (7), 1303 (2025). (in Russian). DOI: 10.61011/JTF.2025.07.60652.54-25
[23] Y. Mishin, D. Farkas, M.J. Mehl, D.A. Papaconstantopoulos. Phys. Rev. B, **59** (5), 3393 (1999).
[24] J. Choi, S. Yoo, S. Song, J.S. Park, K. Kang. J. Mech. Sci. Technol., **32** (7), 3273 (2018).
[25] D.K. Belashchenko. High Temp., **58** (1), 64 (2020). DOI: 10.1134/S0018151X20010034
[26] N.A. Smirnov. J. Appl. Phys., **134** (2), 025901 (2023).
[27] V.K. Kopyshev, A.B. Medvedev. *Obzor printsipial'nykh idei modelei uravnenii sostoyaniya vo VNIIEF*. V sb. *Vysokie plotnosti energii* (RFYaTs–VNIIEF, Sarov, 1997), s. 271–283 (in Russian).
[28] D.N. Nikolaev, A.A. Pyalling, K.V. Khishchenko, V.Ya. Ternovoi, V.E. Fortov. Khim. fizika, **19** (10), 98 (2000) (in Russian).
[29] R.F. Trunin, *Issledovaniya ekstremal'nykh sostoyanii kondensirovannykh veshchestv metodom udarnykh voln. Uravneniya Gyugonio* (RFYaTs-VNIIEF, Sarov, 2006) (in Russian).
[30] M.E. Povarnitsyn, K.V. Khishchenko, P.R. Levashov. Int. J. Impact Eng., **33** (1–12), 625 (2006).
[31] R.K. Bel'kheeva. PMTF, **53** (4), 3 (2012) (in Russian).
[32] R.K. Bel'kheeva. PMTF, **48** (5), 53 (2007) (in Russian).
[33] L.P. Orlenko. *Fizika vzryva i udara* (Fizmatlit, M., 2008) (in Russian).
[34] R.K. Belkheeva. High Temp., **53** (3), 348 (2015). DOI: 10.1134/S0018151X15020054
[35] S.A. Kinelovskii, K.K. Maevskii. Vestnik NGU. Seriya: Fizika, (in Russian) **4** (4), 71 (2009).
[36] S.D. Gilev. FGV, **54** (4), 107 (2018) (in Russian).
[37] A.Yu. Semenov, S.A. Abrosimov, I.A. Stuchebryukhov, K.V. Khishchenko. TVT, **61** (4), 542 (2023) (in Russian).

[38] K.V. Khishchenko. TVT, **35** (6), 1002 (1997) (in Russian).
[39] K.V. Khishchenko. J. Phys.: Conf. Ser., **121**, 022025 (2008).
[40] K.V. Khishchenko. J. Phys.: Conf. Ser., **653**, 012081 (2015).
[41] T.V. Popova, A.E. Mayer, K.V. Khishchenko. J. Appl. Phys., **123**, 235902 (2018).
[42] N.N. Seredkin, K.V. Khishchenko. TVT, **62** (4), 513 (2024) (in Russian). DOI: 10.31857/S0040364424040052
[43] R.I. Nigmatulin. *Osnovy mekhaniki geterogennykh sred* (Nauka, M., 1978) (in Russian).
[44] G.M. Lyakhov. *Osnovy dinamiki vzryvnykh voln v gruntakh i gornykh porodakh* (Nedra, M., 1974) (in Russian).
[45] S.Z. Dunin, V.V. Surkov. PMTF, **5**, 106 (1979) (in Russian).
[46] R.K. Bel'kheeva. TVT, **61** (5), 693 (2023) (in Russian). DOI: 10.31857/S0040364423050022
[47] S.A. Kinelovskii, K.K. Maevskii. High Temp., **54** (5), 675 (2016). DOI: 10.1134/S0018151X16050163
[48] S.A. Kinelovskii, K.K. Maevskii. High Temp., **56** (6), 853 (2018). DOI: 10.1134/S0018151X18060172
[49] K.K. Maevskii. Tech. Phys., **66** (5), 749 (2021). DOI: 10.1134/S1063784221050145
[50] R.F. Trunin, G.V. Simakov, Yu.N. Sutulov, A.B. Medvedev, B.D. Rogozkin, Yu.V. Fedorov. ZhETF, **96** (3), 1024 (1989) (in Russian).
[51] S.B. Kormer, A.I. Funtikov, V.D. Urlin, A.N. Kolesnikova. ZhETF, **42** (3), 686 (1962) (in Russian).
[52] J.M. Walsh, M.H. Rice, R.G. McQueen, F.L. Yarger. Phys. Rev., **108**, 196 (1957).
[53] R.G. McQueen, S.P. Marsh. J. Appl. Phys., **31**, 1253 (1960).
[54] L.V. Al'tshuler, A.A. Bakanova, R.F. Trunin. ZhETF, **42** (1), 717 (1962) (in Russian).
[55] W.H. Isbell, F.H. Shipman, A.H. Jones. *Laboratory Report MSL Material Science 68-13* (General Motors Tech. Center, Warren, MI, 1968)
[56] S.P. Marsh (editor). *LASL Shock Hugoniot Data* (University of California Press, Berkeley, CA, 1980)
[57] L.V. Al'tshuler, A.A. Bakanova, I.P. Dudoladov, E.A. Dynin, R.F. Trunin, B.S. Chekin. PMTF, (2), 3 (1981) (in Russian).
[58] R.F. Trunin, G.V. Simakov. ZhETF, **103** (6), 2180 (1993) (in Russian).
[59] V.K. Gryaznov, M.V. Zhernokletov, I.L. Iosilevskii, G.V. Simakov, R.F. Trunin, L.I. Trusov, V.E. Fortov. ZhETF, **114** (4), 1242 (1998) (in Russian).
[60] D.K. Belashchenko. High Temp., **58** (1), 64 (2020). DOI: 10.1134/S0018151X20010034
[61] I.V. Lomonosov. Laser Part. Beams, **25** (4), 567 (2007). DOI: 10.7868/S0040364417040111
[62] L.F. Gudarenko, O.N. Gushchina, M.V. Zhernokletov, A.B. Medvedev, G.V. Simakov. TVT, **38** (3), 437 (2000) (in Russian).
[63] D.K. Belashchenko. ZhFKh, **94** (10), 1450 (2020) (in Russian). DOI: 10.31857/S0044453720100064
[64] P.R. Levashov, V.E. Fortov, K.V. Khishchenko, I.N. Lomov, I.V. Lomonosov. AIP Conf. Proc. **429**, 47 (1998).
[65] P.R. Levashov, K.V. Khishchenko, I.V. Lomonosov, V.E. Fortov. AIP Conf. Proc., **706**, 87 (2004).
[66] D.K. Belashchenko. *Liquid Metals. From Atomistic Potentials to the Properties, Shock Compression, Earth's Core and Nanoclusters* (Nova Science Publishers, Hauppauge, NY., 2018)
[67] V.V. Yakushev, S.Yu. Anan'ev, A.V. Utkin, A.N. Zhukov, A.Yu. Dolgoborodov. FGV, **54** (5), 45 (2018) (in Russian). DOI: 10.15372/FGV20180506
[68] V.V. Yakushev, S.Yu. Anan'ev, A.V. Utkin, A.N. Zhukov, A.Yu. Dolgoborodov. FGV, **55** (6), 108 (2019) (in Russian). DOI: 10.15372/FGV20190615

Translated by M.Shevelev